Electronic Supplementary Information

Fabricating Ga doped and MgO embedded nanomaterials for sorption-enhanced steam reforming of methanol

Zhao Sun,[a1] Junpeng Liu,[a1] Rongjun Zhang,[c] Yu Wu,[c] Hongwei Li,[c] Sam Toan[b] and Zhiqiang Sun*[a]

[a] School of Energy Science and Engineering, Central South University, Changsha 410083, China

[b] Department of Chemical Engineering, University of Minnesota, Duluth, MN 55812, USA

[c] State Key Laboratory of Catalytic Materials and Reaction Engineering, Research Institute of Petroleum Processing, SINOPEC, Beijing 100083, China

* Corresponding author: zqsun@csu.edu.cn

[1] These authors contribute equally to this work.

The Supporting Information includes:

1. CS characterizations

The XRD patterns of un-reduced *x*GaCuMg CSs are shown in **Fig. S1**. Besides the diffraction peak belongs to MgO (36.9°, 42.9°, 62.2°, 74.6°, and 78.5°) as mentioned above, the diffraction peaks of CuO with the 2θ value of 35.4° and 38.64°, which corresponds the (-111) and (111) plane respectively, can also be observed. The diffraction peaks ascribed to Ga oxide were still not detected, verifying the high dispersion of Ga oxide again.

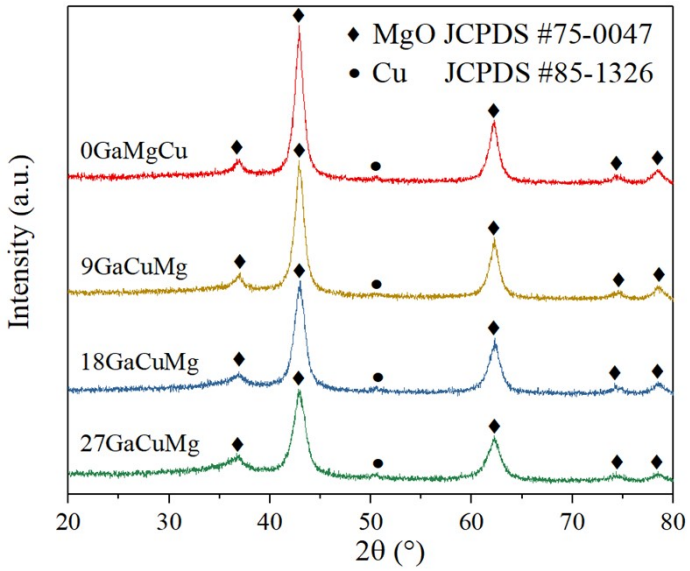

Fig. S1. XRD patterns of un-reduced *x*GaCuMg catalyst.

The H_2-TPR measurements were conducted to investigate the reducibility of Cu species over unreduced *x*GaCuMg CSs, as presented in **Fig. S2**. The reduction temperature and intensity of H_2-TPR curves are different, demonstrating that the Ga doping exerted an effect on the reducibility of Cu species. According to reported literature, the reduction peak located at 150~300°C can be ascribed to the reduction of CuO species which contact intimately with carrier oxide due to the fact that the strong interaction between Cu and carrier oxide can promote the reduction of CuO; the peak

at 300~350°C can be assigned to the poorly interacting and/or larger CuO particles that need to be reduced under higher temperature[1]. All *x*GaCuMg CSs exhibited the low-temperature peak (150~300°C), and the reduction temperature of these peaks decreased with the increasing Ga doping, indicating the copper species were contacted closely with the carrier (mainly Ga_2O_3), and this interaction promoted the reducibility of copper species[2]. The results of H_2-TPR also confirmed the conclusion inferred by XPS. Besides, all samples presented roughly symmetrical narrow peaks, implying the uniform size distribution of copper species in these catalysts.

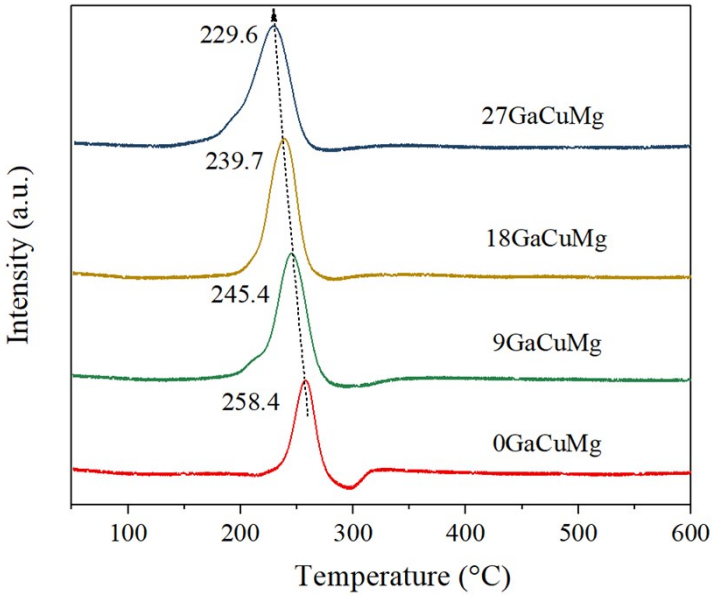

Fig. S2. H_2-TPR profiles of the *x*GaCuMg catalyst.

2. SE-SRM tests

The effects of S/C mole ratio on the SE-SRM performance were shown in **Fig. S3**. It can be seen that the increase of S/C mole ratio is first conducive to improve the H_2 selectivity, which may be due to the fact that an appropriate addition of water could promote the CO_2 absorption performance of Mg-based absorbent via the reaction pathway of MgO→ $Mg(OH)_2$→$MgCO_3$[3]. However, when the S/C ratio achieved 1.75, the CO_2 selectivity increased which was possibly caused by the competitive adsorption between H_2O and CO_2 over catalyst surface[4]. For methanol conversion, a higher S/C ratio could promote the SRM reaction toward H_2 generation and thus improve the methanol conversion, but this improvement became insignificant when the S/C ratio was higher than 1.50. Therefore, the S/C mole ratio of 1.50 was selected as the optimal ratio for the SE-SRM reaction.

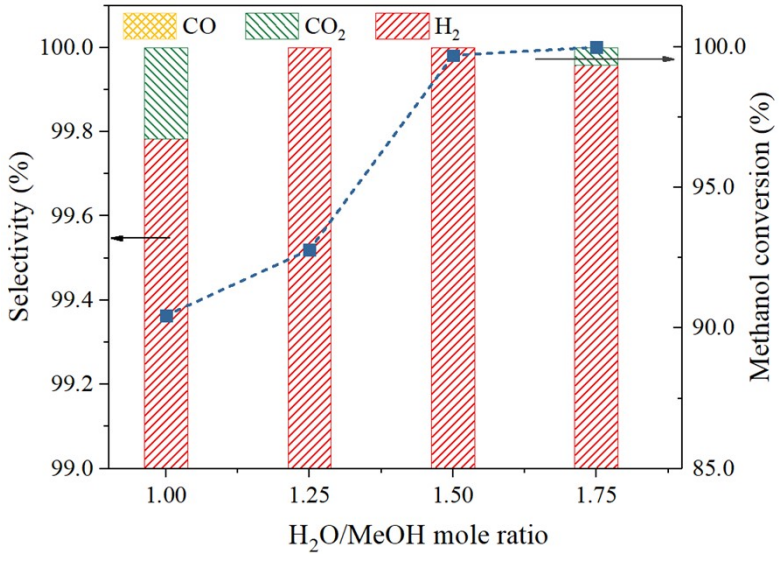

Fig. S3. Effects of H_2O/MeOH mole ratio on H_2, CO_2, and CO selectivity and methanol conversion (Reaction temperature = 200 °C, pressure = 1atm, liquid flow rate = 0.002 mL/min, N_2 flow rate = 40 mL/min).

The effects of reforming temperature on SE-SRM are presented in **Fig. S4**. A

higher reforming temperature was conducive to the conversion of methanol, while it could lead to increases in CO_2 and CO selectivity due to the loss in CO_2 capacity and aggravation of MD and RWGS reactions. It is noted that under the low reaction temperature of 180°C, the 18GaCuMg CS still exhibited a decent SE-SRM performance with the H_2 selectivity, CO_2 selectivity, and methanol conversion of 98.20%, 1.80%, and 91.39%, respectively. Simultaneously, no CO was generated during the reforming process. The results show the great potential of 18GaCuMg CS for low-temperature steam reforming of methanol. Due to the superior SE-SRM performance obtained at 200°C, the reforming temperature of 200°C was seen as the optimal temperature for the SE-SRM reaction.

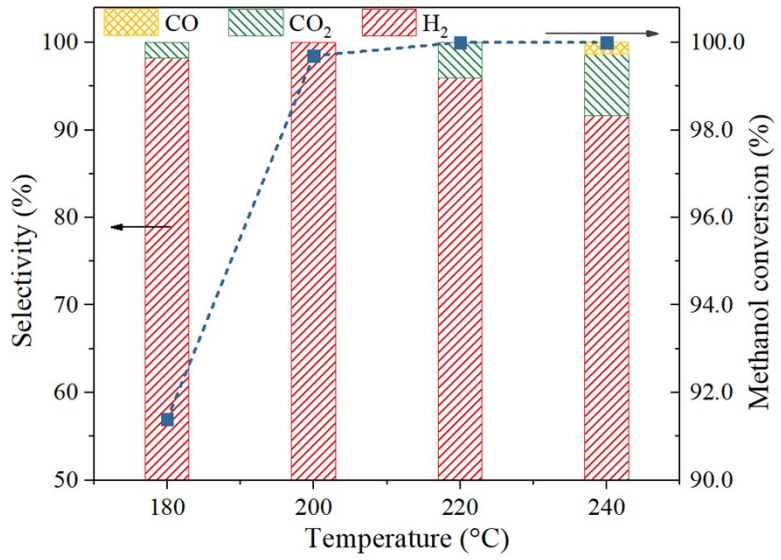

Fig. S4. Effects of reforming temperature on H_2, CO_2, and CO selectivity and methanol conversion (Pressure = 1atm, S/C = 1.5, liquid flow rate = 0.002 mL/min, N_2 flow rate = 40 mL/min).

The detailed SE-SRM performance analysis of 18GaCuMg CS under different feed flow rates (or GHSVs) are discussed below:

As show in **Fig. S5**a, all methanol conversions under the flow rates of 0.002 mL/min, 0.004 mL/min, 0.006 mL/min, and 0.008 mL/min are closed to 99.70%, confirming the high catalytic activity of 18GaCuMg CS. When the flow rate was further increased to 0.01 mL/min, the methanol conversion decreased slightly from 99.70% to 99.40%. For H_2 selectivity, approximate 100% selectivity under flow rates 0.002 mL/min, 0.004 mL/min, 0.006 mL/min, and 0.008 mL/min. When the feed flow rate was further increased, a decrease in H_2 selectivity and an increasement in CO_2 selectivity could be observed, which may be caused by the CO_2 absorption saturation under high feeding flow rates of methanol. The variations for CO selectivity are shown in **Fig. S5**b. At the low flow rate of 0.002 mL/min, no CO was detected. With increase of feeding flow rate, the CO selectivity gradually increased from 0 to approximate 0.06%. Although the formation of CO under high feeding flow rate cannot by inhibited completed, the CO selectivity of 0.06% has been already at a low level in the existing researches [5-7], which is conducive to the utilization by the high-temperature proton exchange membrane fuel cells (PEMFCs).

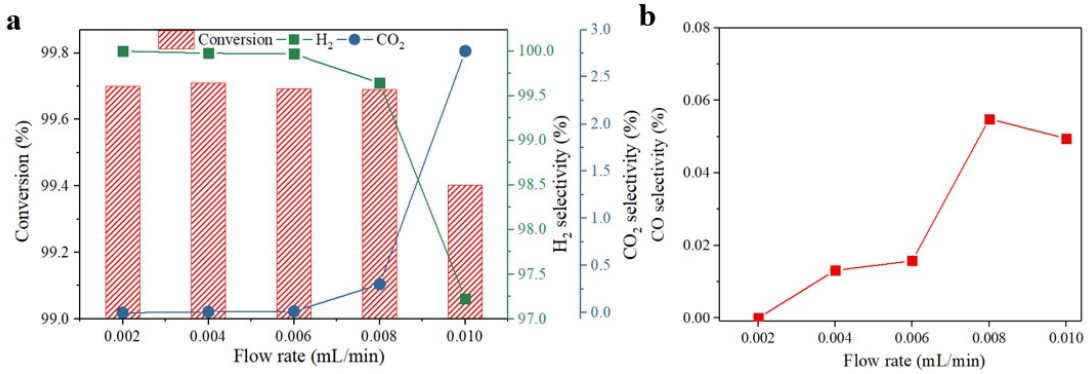

Fig. S5. SE-SRM performance of 18GaCuMg CS at different flow rates: a) methanol conversion, H_2 selectivity, and CO_2 selectivity; b) CO selectivity. (The GHSV values for 0.002 mL/min, 0.004 mL/min, 0.006 mL/min, 0.008 mL/min, and 0.01 mL/min are 2604 h^{-1}, 2708 h^{-1}, 2811 h^{-1}, 2915 h^{-1}, and 3019 h^{-1}, respectively.)

The studies with similar GHSV value were also compared as shown in Fig. 1 and Table 1. It can be seen that, the prepared 18GaCuMg CS can reach a relatively high methanol conversion and hydrogen purity at a lower reforming temperature under the premise of a similar GHSV value, proving its superior activity in SE-SRM process.

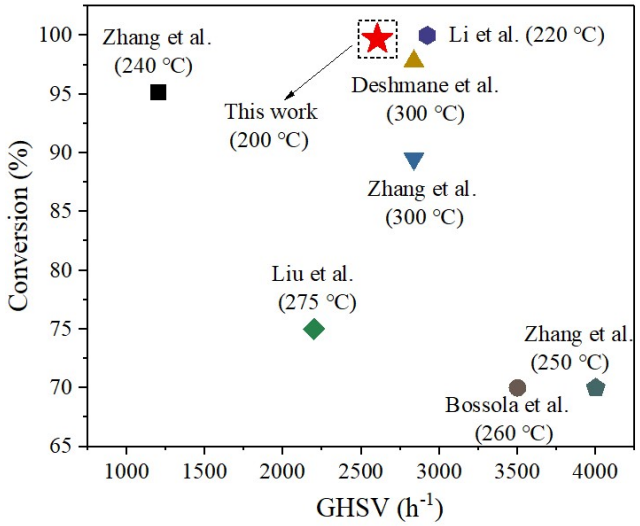

Fig. S6. Different research with similar GHSV values in SRM process and their methanol conversions.

Table S1.

Different research with similar GHSV values in SRM process and their main results.

Catalyst	**Reforming conditions**	**Methanol conversion (%)**	**Reformate (H_2, CO_2, and CO) selectivity (%)**	**Reference**
$Cu/ZnO/CeO_2/ZrO_2$	T=240 °C, S/C=1.2 GHSV=1200 h^{-1}	95.2	H_2=94.6, CO_2=3.6, CO=1.8	[8]
Cu/MCM-41	T=300 °C, S/C=3 GHSV=2838 h^{-1}	89.5	H_2=100, CO_2=98.4, CO=1.6	[9]
Al_2O_3 and ZrO_2 modified $CuO/ZnO/Ga_2O_3$	T=275 °C, S/C=1 GHSV=2200 h^{-1}	75	CO=0.3	[10]
ZrO_2 promoted Cu/ZnO	T=300 °C, S/C=2 GHSV=2838 h^{-1}	97.8	H_2=99.0, CO_2=99.6, CO=0.4	[11]
$Cu/MgO/Al_2O_3$	T=220 °C, S/C=1.3 GHSV=2923 h^{-1}	100	H_2=99.3, CO<0.15	[12]
$Cu/SiO_2/ZrO_2$	T=260 °C, S/C=1.3 GHSV=3500 h^{-1}	70	H_2=75, CO=25. CO≈0	[13]
Cu_2O/ZnO	T=250 °C, S/C=2 GHSV=4000 h^{-1}	70	CO_2=100, CO=0	[14]

3. Mechanism investigation

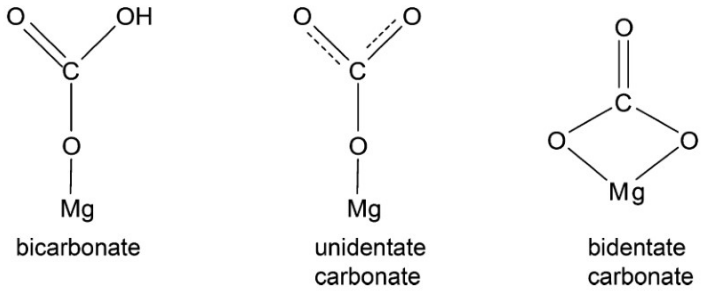

Fig. S7. Three different types of CO_2 absorption modes on MgO: bicarbonate, unidentate carbonate, and bidentate carbonate[15].

Table S2.

Identification of species in the DRIFTS spectra.

Species	Wavenumber (cm^{-1})	Mode	References
$Methanol_{(g)}$	1455	δ_s CH	[16]
$Methoxy_{(ads)}$	1046	v CO	[17]
	2819	v_s CH	[18]
	2929	v_{as} CH	[18]
$Formaldehyde_{(ads)}$	2730/2737	v CH	[19]
$Formate_{(ads)}$	1353	δ CH	[20]
	1622	v OCO_{as}	[20]
	2894	v CH	[21]
$CO_{2(g)}$	2090	v CO (R-branch)	[22]
$CO_{(g)}$	2358	v_{as} CO (R-branch)	[22]
OH	3734	v(OH)	[23]

Explanations: v = stretching, δ = bending vibrations

4. Kinetic analysis

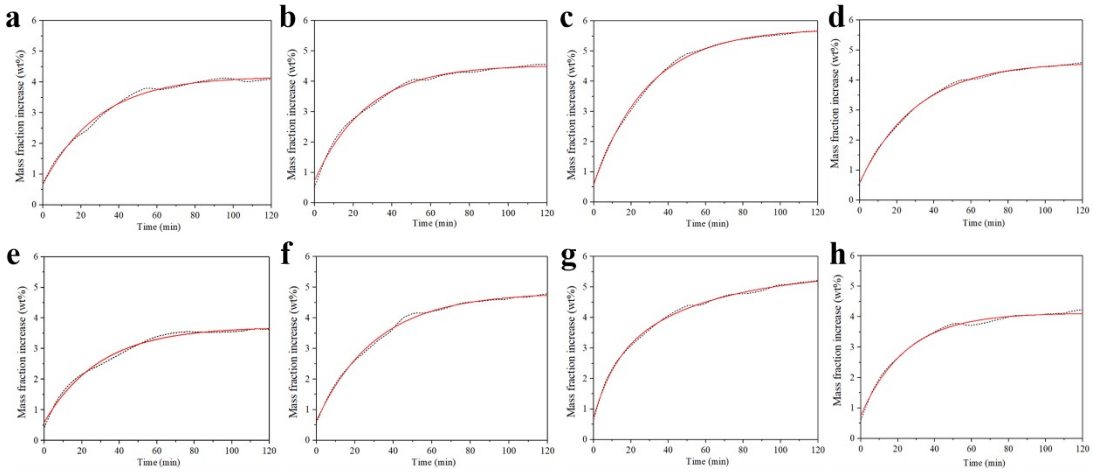

Fig. S8. Comparison of CO_2 uptake curves of CSs (black dotted line) and lines plotted based on the double-exponential model: a) 0GuCuMg, adsorbed at 180°C; b) 0GuCuMg, adsorbed at 200°C; c) 0GuCuMg, adsorbed at 220°C; d) 0GuCuMg, adsorbed at 240°C; e) 18GuCuMg, adsorbed at 180°C; f) 18GuCuMg, adsorbed at 200°C; g) 18GuCuMg, adsorbed at 220°C; h) 18GuCuMg, adsorbed at 240°C.

5. DFT calculations

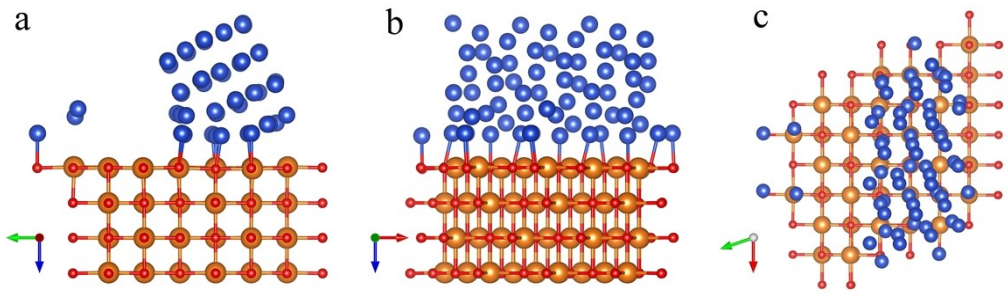

Fig. S9. Configuration of the Cu(111)/MgO(200) module. a) main view; b) side view; and c) top view.

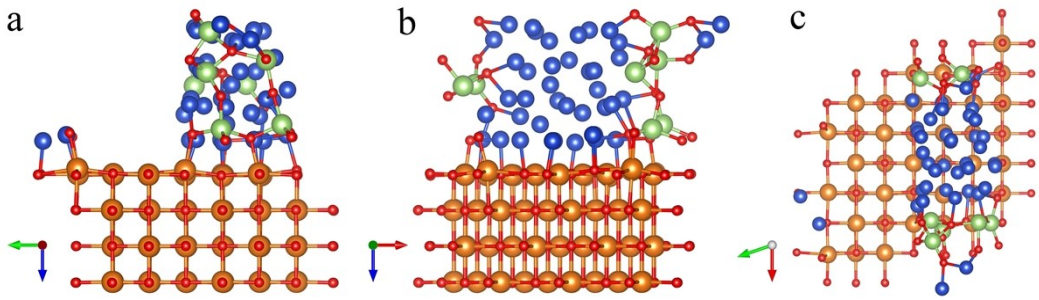

Fig. S10. Configuration of the Cu(111)/Ga_2O_3(202)/MgO(200) module. a) main view; b) side view; and c) top view.

References

[1] C. Mateos-Pedrero, H. Silva, D.A. Pacheco Tanaka, S. Liguori, A. Iulianelli, A. Basile, A. Mendes, CuO/ZnO catalysts for methanol steam reforming: The role of the support polarity ratio and surface area, Appl. Catal. B-Environ., 174-175 (2015) 67-76.

[2] W. Tong, K. Cheung, A. West, K.-M. Yu, S.C.E. Tsang, Direct methanol steam reforming to hydrogen over $CuZnGaO_x$ catalysts without CO post-treatment: mechanistic considerations, Phy. Chem. Chem. Phys., 15 (2013) 7240-7248.

[3] Y. Hu, Y. Guo, J. Sun, H. Li, W. Liu, Progress in MgO sorbents for cyclic CO_2 capture: a comprehensive review, J. Mater. Chem. A, 7 (2019) 20103-20120.

[4] Y. Wang, M.Z. Memon, M.A. Seelro, W. Fu, Y. Gao, Y. Dong, G. Ji, A review of CO_2 sorbents for promoting hydrogen production in the sorption-enhanced steam reforming process, Int. J. Hydrogen Energ., 46 (2021) 23358-23379.

[5] Sun Z, Sun ZQ. Hydrogen generation from methanol reforming for fuel cell applications - A review. J. Cent. South Univ., 2020; 27(4): 1074-1103.

[6] Mateos-Pedrero C, Azenha C, Pacheco Tanaka DA, Sousa JM, Mendes A. The influence of the support composition on the physicochemical and catalytic properties of Cu catalysts supported on Zirconia-Alumina for methanol steam reforming. Appl. Catal. B-Environ., 2020: 277: 119243.

[7] Li HZ, Ma C, Zou XY, Huang Z, Zhu L. On-board methanol catalytic reforming for hydrogen Production - A review. Int. J. Hydrogen Energ., 2021; 46(43): 22303-22327.

[8] Zhang L, J-t Lei, Yuan T, Xin H, Jin B, Dan L, et al. Effect of precursor and precipitant concentrations on the catalytic properties of CuO/ZnO/CeO_2-ZrO_2 for methanol steam reforming. J. Fuel Chem. Tech., 2015; 43: 1366-1374.

[9] Deshmane VG, Abrokwah RY, Kuila D. Synthesis of stableCu-MCM-41 nano catalysts for H_2 production with high selectivity via steam reforming of methanol. International Journal of Hydrogen Energy, 2015; 40:10439.

[10] Liu X, Toyir J, Priscina P. Homs N. Hydrogen production from methanol steam reforming over Al_2O_3- and ZrO_2-modified CuOZnOGa_2O_3 catalysts. Int. J.

Hydrogen Energ., 2017, 42: 13704-13711.

[11] Mohtashami Y, Taghhizadeh M. Performance of the ZrO_2 promoted CueZnO catalyst supported on acetic acid-treated MCM-41 in methanol steam reforming. Int. J. Hydrogen Energ., 2019, 44: 5725-5738.

[12] Li H, Tian H, Chen S, Sun Z, Liu T, Liu R, Assabumrugrat S, Saupsor H, Mu R, Pei C, Gong J. Sorption enhanced steam reforming of methanol for high-purity hydrogen production over Cu-MgO/Al_2O_3 bifunctional catalysts. Appl. Catal. B-Environ., 2020, 276: 119052.

[13] Bossola F, Scotti N, Somodi F, Coduri M, Evangelisti C, Santo V. Electron-poor copper nanoparticles over amorphous zirconia-silica as all-inone catalytic sites for the methanol steam reforming. Appl. Catal. B-Environ., 2019, 258: 118016.

[14] Zhang G, Zhao J, Yang T, Zhang Q, Zhang L. In-situ self-assembled Cu_2O/ZnO core-shell catalysts synergistically enhance the durability of methanol steam reforming. Appl. Catal. B-Gen., 2021, 616: 118072.

[15] P. Li, R. Chen, Y. Lin, W. Li. General approach to facile synthesis of MgO-based porous ultrathin nanosheets enabling high-efficiency CO_2 capture. Chem. Eng. J., 2021, 404: 126459.

[16] K. Ploner, M. Watschinger, P.D. Kheyrollahi Nezhad, T. Götsch, L. Schlicker, E.-M. Köck, A. Gurlo, A. Gili, A. Doran, L. Zhang, N. Köwitsch, M. Armbrüster, S. Vanicek, W. Wallisch, C. Thurner, B. Klötzer, S. Penner, Mechanistic insights into the catalytic methanol steam reforming performance of Cu/ZrO_2 catalysts by in situ and operando studies, J. Catal., 391 (2020) 497-512.

[17] H. Li, H. Tian, S. Chen, Z. Sun, T. Liu, R. Liu, S. Assabumrungrat, J. Saupsor, R. Mu, C. Pei, J. Gong, Sorption enhanced steam reforming of methanol for high-purity hydrogen production over Cu-MgO/Al_2O_3 bifunctional catalysts, Appl. Catal. B-Environ., 276 (2020) 119052.

[18] J. Toyir, P. Ramirez de la Piscina, N. Homs. Ga-promoted copper-based catalysts highly selective for methanol steam reforming to hydrogen; relation with the hydrogenation of CO_2 to methanol. Int. J. Hydrogen Energ., 2015, 40, 11261-11266.

[19] T. Nakanaga, S. Kondo, S. Saeki. Infrared band intensities of formaldehyde and formaldehyde-d_2. J. Chem. Phys., 1982, 76(8): 3860-3865.

[20] A. Kaftan, M. Kusche, M. Laurin, P. Wasserscheid, J. Libuda, KOH-promoted Pt/Al_2O_3 catalysts for water gas shift and methanol steam reforming: An operando DRIFTS-MS study, Appl. Catal. B-Environ., 201 (2017) 169-181.

[21] J. Toyir, P. Ramirez de la Piscina, N. Homs, Ga-promoted copper-based catalysts highly selective for methanol steam reforming to hydrogen; relation with the hydrogenation of CO_2 to methanol, Int. J. Hydrogen Energ., 40 (2015) 11261-11266.

[22] P. Li, R. Chen, Y. Lin, W. Li, General approach to facile synthesis of MgO-based porous ultrathin nanosheets enabling high-efficiency CO_2 capture, Chem. Eng. J., 404 (2021) 126459.

[23] K. Huttunrn, D. Labadini, S. Hafiz, S. Gokalp, E. Wolff, S. Martel, M. Foster. DRIFTS investigation of methanol oxidation on CeO_2 nanoparticles, Appl. Surf.

Sci., 2021, 554, 149518.